Compositeness of the strange, charm, and beauty odd parity Λ states

C. Garcia-Recio,[1] C. Hidalgo-Duque,[2] J. Nieves,[2] L. L. Salcedo,[1] and L. Tolos[3,4]

[1]*Departamento de Física Atómica, Molecular y Nuclear, and Instituto Carlos I de Física Teórica y Computacional, Universidad de Granada, E-18071 Granada, Spain*

[2]*Instituto de Física Corpuscular (IFIC), Centro Mixto CSIC-Universidad de Valencia, Institutos de Investigación de Paterna, Apartado 22085, E-46071 Valencia, Spain*

[3]*Instituto de Ciencias del Espacio (IEEC/CSIC), Campus Universitat Autònoma de Barcelona, Carrer de Can Magrans, s/n, 08193 Cerdanyola del Vallès, Spain*

[4]*Frankfurt Institute for Advanced Studies, Johann Wolfgang Goethe University, Ruth-Moufang-Straße 1, 60438 Frankfurt am Main, Germany*

(Received 16 June 2015; published 11 August 2015)

We study the dependence on the quark mass of the compositeness of the lowest-lying odd parity hyperon states. Thus, we pay attention to Λ-like states in the strange, charm, and beauty sectors which are dynamically generated using a unitarized meson-baryon model. In the strange sector we use a SU(6) extension of the Weinberg-Tomozawa meson-baryon interaction, and we further implement the heavy-quark spin symmetry to construct the meson-baryon interaction when charmed or beauty hadrons are involved. In the three examined flavor sectors, we obtain two $J^P = 1/2^-$ and one $J^P = 3/2^-$ Λ states. We find that the Λ states which are bound states (the three Λ_b) or narrow resonances [one $\Lambda(1405)$ and one $\Lambda_c(2595)$] are well described as molecular states composed of s-wave meson-baryon pairs. The $\frac{1}{2}^-$ wide $\Lambda(1405)$ and $\Lambda_c(2595)$ as well as the $\frac{3}{2}^-$ $\Lambda(1520)$ and $\Lambda_c(2625)$ states display smaller compositeness so they would require new mechanisms, such as d-wave interactions.

DOI: 10.1103/PhysRevD.92.034011 PACS numbers: 14.20.Gk, 14.20.Pt, 11.10.St

I. INTRODUCTION

One of the chief theoretical efforts in hadron physics is to understand the nature of hadrons, whether they can be primarily explained within the quark-model picture as multiquark states or mainly qualify as dynamically generated states via hadron-hadron scattering processes. In particular, in the last years there has been a growing interest in the properties of strange and charmed baryons in connection with many experiments such as the ongoing CLEO [1], Belle [2], BES [3], *BABAR* [4] as well as the planned PANDA [5] or the J-PARC upgrade [6]. Also, the LHCb Collaboration at CERN has been exploring in the recent years an almost *terra incognita* in the spectroscopy of baryons with the beauty degree of freedom. Results on beauty baryonic states, such as the Λ_b excited states [7], have been reported, stimulating the theoretical work to understand the properties of the newly discovered states.

Recent approaches based on unitarized coupled-channels methods have proven to be very successful in describing the existing experimental data in the charmed [8–25] and beauty baryonic sectors [26,27]. Most of these models emerge as the theoretical effort extends from the strange to charmed and beauty sectors, partially motivated by the parallelism between the $\Lambda(1405)$ and the $\Lambda_c(2595)$ as well as the $\Lambda_b(5912)$ states. Of special importance are the symmetries that are implemented in the hadronic models. While chiral symmetry should be implemented in the strangeness sector, heavy-quark spin symmetry (HQSS) [28–30] appears naturally as we deal with systems that include charmed and beauty degrees of freedom [31–41].

The use of the effective models combined with unitarity constraints in coupled channels allows us to explain many baryons in terms of meson-baryon interactions, interpreting them as composite or dynamically generated states. The ultimate goal is to determine the degree of "compositeness" and the "genuine" contributions of the given state. The formalism was developed by Weinberg in Ref. [42], and later applied to the deuteron in [43], showing that the deuteron can be fully understood as a proton-neutron bound state. More recent works have extended this analysis from bound states to resonances and from s-wave to higher partial waves [44–51]. The theoretical aspects have been further discussed in [52–54].

The present paper is focused on the analysis of the compositeness of the lowest-lying $J^P = 1/2^-$ and $J^P = 3/2^-$ Λ states going from the strange to the beauty sectors.[1] The aim is to shed some light on the nature of newly discovered excited Λ_c and Λ_b by exploiting the similarities with the strange Λ states. We also address any existing regularity in the quark mass dependence of the compositeness of these excited baryons.

There exist previous studies in the strange sector. The $\Lambda(1520)$ has been recently discussed in Ref. [55], while the

[1]From here on we shall use Λ to indistinctly denote the Λ, Λ_c and Λ_b states.

compositeness and elementariness of the two $\Lambda(1405)$ states have been evaluated within the chiral unitarity model (Goldstone boson-baryon chiral perturbation potential used as a kernel of a Bethe-Salpeter equation) at leading order (Weinberg-Tomozawa interaction) in Ref. [56] and incorporating next-to-leading chiral corrections [57]. While the results reported in Refs. [56,57] are in qualitative agreement with those obtained in this work, there are some appreciable differences between our approach and that followed in [55] for the $\Lambda(1520)$ resonance, namely the consideration of d-wave interactions, whose effects will be further investigated.

The structure of this work is as follows. In Sec. II we summarize the model we are using to describe meson-baryon interactions and present the dynamically-generated Λ resonances in the strange, charm and beauty sectors. In Sec. III we use the generalized Weinberg's sum rule to estimate the importance of the different channels in the generated Λ states. With this analysis, we give an educated guess of the compositeness of these states. Finally, some conclusions are addressed in Sec. IV. In Appendix A we present the analytical expression of compositeness on the first and second Riemann sheets, whereas in Appendix B the compositeness rule is derived.

II. DYNAMICALLY GENERATED STRANGE, CHARM AND BEAUTY Λ STATES

In order to study their compositeness we construct the Λ (isoscalar) states in the strange, charm or beauty sectors as resonances or bound states through a unitarized coupled-channels approach. The channels are composed of meson-baryon pairs interacting in s-wave. We include all ground state mesons with spin-parity 0^- or 1^-, and ground state baryons with $1/2^+$ and $3/2^+$. For the interaction we take an extended Weinberg-Tomozawa (WT) interaction developed in previous works, for the three light flavors in [58–63] and for heavy flavors in [31–35]. The model enjoys chiral and spin-flavor symmetries in the light quark sector and HQSS in the heavy-quark sector.

For completeness we briefly summarize the interaction model here. Further information can be found in [35,58,59,61,63]. The old quark model based on SU(6) spin-flavor symmetry [64–66] enjoyed several successes in correlating hadronic data [67], although eventually it was abandoned in favor of the emerging QCD. In the late nineties it was found that, for baryons, spin-flavor symmetry becomes in fact exact in the limit of large numbers of colors [68]. For the three light flavors the ground state baryons, in this limit, are the $1/2^+$ octet of the nucleon and the $3/2^+$ decuplet of the Δ resonance, and together form the representation **56** of SU(6). No similar result holds for mesons, which fall in the representations **35** and **1** of SU(6), corresponding to the 0^- and 1^- ground state mesons. The significantly different mass of pion and ρ mesons would indicate that spin-flavor is badly broken in this meson sector. However, in two insightful papers [69,70] Caldi and Pagels showed that the vector mesons could be regarded as (dormant) Goldstone boson of the spin-flavor extended chiral group $(\mathrm{SU}(6)_L \times \mathrm{SU}(6)_R)$. This symmetry would exist in the nonrelativistic limit and it is explicitly broken by relativistic corrections which are responsible for the vector meson masses. Several consequences of the Caldi-Pagels scenario have been verified and in particular the collective nature of the ρ meson has been exposed in lattice calculations by Smit [71]. Therefore, while spin-flavor symmetry is not manifest at the level of meson masses, it can be expected that it gives valuable guidance for the classification of the states as well as on the hadronic interactions. Furthermore, as we will see, this symmetry blends nicely with the spin-flavor independence in the heavy quark sector. In order to fix the interaction, we observe that the WT term completely fixes the low-energy interaction of pseudo-Nambu-Goldstone bosons off targets carrying isospin (or in non singlet representations for more than two flavors) [72,73]. As it turns out, the WT interaction is consistent with spin-flavor when the pseudoscalar mesons are coupled with baryons in the **56**, and moreover, the extension of the WT interaction to include vector mesons consistently with spin-flavor exists and it is unique [58,59]. (In retrospective, one can see that this is a consequence of the unique extension of the chiral group $\mathrm{SU}(3)_L \times \mathrm{SU}(3)_R$ to $\mathrm{SU}(6)_L \times \mathrm{SU}(6)_R$ anticipated in [69,70].) In this way we end up with an interaction in the light quark sector consistent with chiral symmetry and spin-flavor symmetry. This approach has shown a reasonable semiqualitative outcome for excited odd-parity baryonic states as compared to the experimental data [62], and also for excited even-parity mesons [61,63].

Turning now to the heavy-quark sector, the key symmetry here is HQSS: in the limit of heavy quark mass, the QCD interaction becomes independent of the spin state of the heavy quark [28–30]. The obvious approach would be to use a similar interaction as for the light sector with more flavors. Once again, although SU(4) flavor symmetry is broken at the level of masses it is routinely used as guidance for the values of the new couplings. In channels without hidden charm or beauty (i.e., without $c\bar{c}$ or $b\bar{b}$ pairs) the direct extension of the previous WT interaction to the heavy sector automatically fulfills HQSS. However, in sectors with hidden charm (or beauty) the interaction is not directly consistent with HQSS. The reason is that spin-flavor only guarantees invariance under spin rotations which are independent for each flavor, but common to quarks and antiquarks of the same flavor. Instead, HQSS requires invariance under independent spin rotations of the heavy quark and the heavy antiquark. Inspection of the WT interaction shows that the offending terms come from OZI suppressed interaction mechanisms involving heavy quark-antiquark pair creation or annihilation. Once these terms are

removed the interaction automatically complies with HQSS. In the process flavor SU(4) is broken [35].

In summary, the model we use to construct the excited odd-parity baryons nicely fulfills the required symmetries in the light and heavy sectors. The symmetries are explicitly broken at the level of masses and decay constants of the basic hadrons. Due to the underlying group structure the model possesses no free parameters, except those induced through hadron loop ultraviolet divergences.

The extended WT meson-baryon interaction, in the coupled meson-baryon basis with total heavy content (charm C / beauty B) H, strangeness S, isospin I and spin J, is given by

$$V_{ij}^{HSIJ} = D_{ij}^{HSIJ} \frac{2\sqrt{s} - M_i - M_j}{4 f_i f_j} \sqrt{\frac{E_i + M_i}{2M_i}} \sqrt{\frac{E_j + M_j}{2M_j}}, \tag{1}$$

where $\sqrt{s}$ is the center of mass (CM) energy of the system; E_i and M_i are, respectively, the CM on-shell energy and mass of the baryon in the channel i; and f_i is the decay constant of the meson in the i-channel. Symmetry breaking effects are introduced by using physical masses and decay constants. The masses and decay constants used in this work are shown in Table I. The masses shown correspond to the arithmetic mean of the different isospin partners.

The D_{ij}^{HSIJ} are the matrix elements coming from the group structure of the extended WT interaction [35]. The matrix elements required for the $\Lambda(1520)$ sector, with quantum numbers $C=0, B=0, S=-1, I=0, J^P=3/2^-$, can be found in Eq. (45) of Ref. [60]. Those for the $\Lambda_c(2595)$, with $C=1, B=0, S=0, I=0, J^P=1/2^-$ and $\Lambda_c(2625)$, with $J^P=3/2^-$, can be found in Tables XV and XVIII of Ref. [31], respectively. The same coefficients apply to the bottom case. Finally, the matrix elements for the $\Lambda(1405)$ sector, with quantum numbers $C=0, B=0, S=-1, I=0, J^P=1/2^-$, can be extracted following the directions of Appendix A of Ref. [62] and the conventions in [74]. For convenience these matrix elements are explicitly displayed in Table II.

In order to obtain the unitarized T-matrix, we solve the on-shell factorized form of the Bethe-Salpeter equation using the matrix V^{HSIJ} as kernel

$$T^{HSIJ} = (1 - V^{HSIJ} G^{HSIJ})^{-1} V^{HSIJ}, \tag{2}$$

where G^{HSIJ} is a diagonal matrix containing the meson-baryon propagator in each channel. Explicitly,

$$G_i^{HSIJ}(\sqrt{s}, m_i, M_i) = i 2 M_i \int \frac{d^4 q}{(2\pi)^4} \frac{1}{q^2 - m_i^2} \frac{1}{(P-q)^2 - M_i^2}, \tag{3}$$

being $M_i(m_i)$ the baryon (meson) mass of the channel i and P^μ the total four-momentum, which in the CM frame is given by $P^\mu_{\rm CM} = (\sqrt{s}, \mathbf{0})$. The loop function is explicitly given in Ref. [75] and in Appendix A.

TABLE I. Baryon masses, M_i, meson masses, m_i, and meson decay constants, f_i, (in MeV) used throughout this work. The widths in MeV units, Γ_R, used in the convolutions [Eq. (4)] are also provided. The masses and decay constants are taken from Refs. [31,34]. The $SU(6) \times SU_C(2) \times U_C(1)$ and $SU(3) \times SU(2)$ labels are displayed as well (for simplicity we do not explicitly give the spin of the heavy quark sector, since it is trivially 0 or 1/2). The last column indicates the HQSS multiplets. Members of a doublet are placed in consecutive rows.

Meson	Mass	Width	Decay constant	$SU(6)_{U_C(1)}$	$SU(3)_{2J+1}$	HQSS	Baryon	Mass	Width	$SU(6)_{U_C(1)}$	$SU(3)_{2J+1}$	HQSS
π	138.04		92.4	$\mathbf{35_0}$	$\mathbf{8_1}$	singlet	N	938.92		$\mathbf{56_0}$	$\mathbf{8_2}$	singlet
K	495.65		113.0	$\mathbf{35_0}$	$\mathbf{8_1}$	singlet	Λ	1115.68		$\mathbf{56_0}$	$\mathbf{8_2}$	singlet
η	547.86		111.0	$\mathbf{35_0}$	$\mathbf{8_1}$	singlet	Σ	1193.15		$\mathbf{56_0}$	$\mathbf{8_2}$	singlet
ρ	775.49	150	153.0	$\mathbf{35_0}$	$\mathbf{8_3}$	singlet	Ξ	1318.29		$\mathbf{56_0}$	$\mathbf{8_2}$	singlet
K^*	893.88	50	153.0	$\mathbf{35_0}$	$\mathbf{8_3}$	singlet	Σ^*	1382.80	35	$\mathbf{56_0}$	$\mathbf{10_4}$	singlet
ω	782.65		138.0	$\mathbf{35_0}$	ideal	singlet	Ξ^*	1531.80		$\mathbf{56_0}$	$\mathbf{10_4}$	singlet
ϕ	1019.46		163.0	$\mathbf{35_0}$	ideal	singlet	Λ_c	2286.46		$\mathbf{21_1}$	$\mathbf{3_2^*}$	singlet
η'	957.78		111.0	$\mathbf{1_0}$	$\mathbf{1_1}$	singlet	Ξ_c	2469.34		$\mathbf{21_1}$	$\mathbf{3_2^*}$	singlet
D	1867.23		157.4	$\mathbf{6_1^*}$	$\mathbf{3_1^*}$	doublet	Σ_c	2453.54		$\mathbf{21_1}$	$\mathbf{6_2}$	doublet
D^*	2008.61		f_D	$\mathbf{6_1^*}$	$\mathbf{3_3^*}$	doublet	Σ_c^*	2518.07		$\mathbf{21_1}$	$\mathbf{6_4}$	doublet
D_s	1968.30		193.7	$\mathbf{6_1^*}$	$\mathbf{3_1^*}$	doublet	Ξ_c'	2576.75		$\mathbf{21_1}$	$\mathbf{6_2}$	doublet
D_s^*	2112.10		f_{D_s}	$\mathbf{6_1^*}$	$\mathbf{3_3^*}$	doublet	Ξ_c^*	2645.90		$\mathbf{21_1}$	$\mathbf{6_4}$	doublet
B	5279.42		133.6	$\mathbf{6_1^*}$	$\mathbf{3_1^*}$	doublet	Λ_b	5619.50		$\mathbf{21_1}$	$\mathbf{3_2}$	singlet
B^*	5325.20		f_B	$\mathbf{6_1^*}$	$\mathbf{3_3^*}$	doublet	Ξ_b	5794.00		$\mathbf{21_1}$	$\mathbf{3_2^*}$	singlet
B_s	5366.77		159.1	$\mathbf{6_1^*}$	$\mathbf{3_1^*}$	doublet	Σ_b	5813.40		$\mathbf{21_1}$	$\mathbf{6_2}$	doublet
B_s^*	5415.40		f_{B_s}	$\mathbf{6_1^*}$	$\mathbf{3_3^*}$	doublet	Σ_b^*	5833.60		$\mathbf{21_1}$	$\mathbf{6_4}$	doublet
							Ξ_b'	5926.00		$\mathbf{21_1}$	$\mathbf{6_2}$	doublet
							Ξ_b^*	5949.30		$\mathbf{21_1}$	$\mathbf{6_4}$	doublet

TABLE II. Matrix elements D_{ij} for the $\Lambda(1405)$ sector: $C = B = 0, S = -1, I = 0, J^P = 1/2^-$.

	$\Sigma\pi$	$N\bar{K}$	$\Lambda\eta$	ΞK	$N\bar{K}^*$	$\Lambda\omega$	$\Sigma\rho$	$\Lambda\phi$	$\Sigma^*\rho$	ΞK^*	$\Xi^* K^*$
$\Sigma\pi$	-4	$\sqrt{\frac{3}{2}}$	0	$-\sqrt{\frac{3}{2}}$	$\sqrt{\frac{1}{2}}$	0	$\sqrt{\frac{64}{3}}$	0	$\sqrt{\frac{32}{3}}$	$\sqrt{\frac{25}{2}}$	2
$N\bar{K}$	$\sqrt{\frac{3}{2}}$	-3	$-\sqrt{\frac{9}{2}}$	0	$\sqrt{27}$	$\sqrt{\frac{9}{2}}$	$\sqrt{\frac{1}{2}}$	3	2	0	0
$\Lambda\eta$	0	$-\sqrt{\frac{9}{2}}$	0	$\sqrt{\frac{9}{2}}$	$\sqrt{\frac{27}{2}}$	0	0	0	0	$-\sqrt{\frac{3}{2}}$	$\sqrt{12}$
ΞK	$-\sqrt{\frac{3}{2}}$	0	$\sqrt{\frac{9}{2}}$	-3	0	$-\sqrt{\frac{1}{2}}$	$\sqrt{\frac{25}{2}}$	-1	-2	$\sqrt{3}$	0
$N\bar{K}^*$	$\sqrt{\frac{1}{2}}$	$\sqrt{27}$	$\sqrt{\frac{27}{2}}$	0	-9	$\sqrt{\frac{3}{2}}$	$\sqrt{\frac{25}{6}}$	$-\sqrt{27}$	$-\sqrt{\frac{4}{3}}$	0	0
$\Lambda\omega$	0	$\sqrt{\frac{9}{2}}$	0	$-\sqrt{\frac{1}{2}}$	$\sqrt{\frac{3}{2}}$	0	4	0	$\sqrt{8}$	$\sqrt{\frac{25}{6}}$	$\sqrt{\frac{4}{3}}$
$\Sigma\rho$	$\sqrt{\frac{64}{3}}$	$\sqrt{\frac{1}{2}}$	0	$\sqrt{\frac{25}{2}}$	$\sqrt{\frac{25}{6}}$	4	$-\frac{20}{3}$	0	$\sqrt{\frac{8}{9}}$	$-\sqrt{\frac{169}{6}}$	$\sqrt{\frac{4}{3}}$
$\Lambda\phi$	0	3	0	-1	$-\sqrt{27}$	0	0	-4	0	$\sqrt{\frac{1}{3}}$	$-\sqrt{\frac{8}{3}}$
$\Sigma^*\rho$	$\sqrt{\frac{32}{3}}$	2	0	-2	$-\sqrt{\frac{4}{3}}$	$\sqrt{8}$	$\sqrt{\frac{8}{9}}$	0	$-\frac{22}{3}$	$-\sqrt{\frac{4}{3}}$	$-\sqrt{\frac{128}{3}}$
ΞK^*	$\sqrt{\frac{25}{2}}$	0	$-\sqrt{\frac{3}{2}}$	$\sqrt{3}$	0	$\sqrt{\frac{25}{6}}$	$-\sqrt{\frac{169}{6}}$	$\sqrt{\frac{1}{3}}$	$-\sqrt{\frac{4}{3}}$	$-\frac{19}{3}$	$-\sqrt{\frac{32}{9}}$
$\Xi^* K^*$	2	0	$\sqrt{12}$	0	0	$\sqrt{\frac{4}{3}}$	$\sqrt{\frac{4}{3}}$	$-\sqrt{\frac{8}{3}}$	$-\sqrt{\frac{128}{3}}$	$-\sqrt{\frac{32}{9}}$	$-\frac{14}{3}$

When the meson and/or the baryon in the intermediate state is not a stable particle, we convolute the meson-baryon propagator (loop) with the corresponding hadronic spectral function, as done in Refs. [32,76,77]. Thus, in this case, the loop function G is substituted by $\hat{G}$, which is defined as the convolution of the loop function G with the spectral function of this intermediate resonant state (R),

$$\hat{G}^{HSIJ}(\sqrt{s}, m, M_R, \Gamma_R) = \frac{1}{N}\int_{(M_R-2\Gamma_R)^2}^{(M_R+2\Gamma_R)^2} d\hat{M}^2 \left(-\frac{1}{\pi}\right) \mathrm{Im}\left(\frac{1}{\hat{M}^2 - M_R^2 + iM_R\Gamma_R}\right) \times G^{HSIJ}(\sqrt{s}, m, \hat{M}), \tag{4}$$

being N a normalization factor that reads,

$$N = \int_{(M_R-2\Gamma_R)^2}^{(M_R+2\Gamma_R)^2} d\hat{M}^2 \left(-\frac{1}{\pi}\right) \mathrm{Im}\left(\frac{1}{\hat{M}^2 - M_R^2 + iM_R\Gamma_R}\right). \tag{5}$$

The meson-baryon propagator is logarithmically ultraviolet divergent, thus, it needs to be renormalized. This has been done by a subtraction point regularization such that

$$G_{ii}^{HSIJ}(\sqrt{s}) = 0 \quad \text{at} \quad \sqrt{s} = \mu^{HSI}, \tag{6}$$

with

$$\mu^{HSI} = \sqrt{\alpha}\sqrt{m_{\mathrm{th}}^2 + M_{\mathrm{th}}^2}, \tag{7}$$

where m_{th} and M_{th}, are, respectively, the masses of the meson and baryon producing the lowest threshold (minimal value of $m_{\mathrm{th}} + M_{\mathrm{th}}$) for each HSI sector, independent of the angular momentum J, and $\alpha = 1$. This renormalization scheme was first proposed in Refs. [12,13] and it was successfully used in Refs. [31–35,78]. A recent discussion on the regularization method can be found in Ref. [79]. The overall results obtained by the above choice of subtraction point is similar to the observed spectrum of low-lying hadronic resonances. A more precise agreement can be achieved by suitably shifting the subtraction point. To do so one can choose a value of the parameter α different from unity [31,34]. Note that, other than this, the model has no free parameters.

The dynamically-generated baryon states appear as poles of the scattering amplitudes on the complex energy $\sqrt{s}$ plane. The poles of the scattering amplitude on the first Riemann sheet that appear on the real axis below threshold are interpreted as *bound states*. The poles that are found on the second Riemann sheet below the real axis and above threshold are identified with *resonances*.[2] The mass and the width of the state can be found from the position of the pole on the complex energy plane. Close to the pole, the scattering amplitude behaves as

$$T_{ij}^{HSIJ}(s) \approx \frac{g_i g_j}{\sqrt{s} - \sqrt{s_R}}. \tag{8}$$

The mass M_R and width Γ_R of the state result from $\sqrt{s_R} = M_R - \mathrm{i}\Gamma_R/2$, while g_j (complex in general) is the coupling of the state to the j-channel.

The calculated positions and widths of the lowest-lying Λ states in the strange, charm and beauty sectors together

[2]For convenience we will often use the word resonance for all molecular states discussed in this work, whether they are bound states or proper resonances.

TABLE III. Calculated masses, widths and compositeness of the negative-parity Λ states in the strange sector. The coupling constants and the weights of the various channels are also displayed. The main numbers refer to the default value $\alpha = 1$, while the numbers in parenthesis refer to the same quantities computed with a subtraction point chosen so that the masses are close to the experimental ones [80]. For this purpose similar masses have been adopted for the two $\Lambda(\frac{1}{2}^-)$ states. For each Λ state the largest compositeness weights have been highlighted with boldface.

State	J^P	$\sqrt{\alpha}$	M_R	Γ_R	$1-Z$	Channel	$\lvert g_i\rvert$	g_i	X_i	(X_i)
$\Lambda(1405)$	$\frac{1}{2}^-$	1	1430.0	5.5	0.887	$\pi\Sigma$	0.50	$0.19+0.46i$	−0.008	(−0.006)
		(0.867)	(1405.1)	(12.8)	(0.772)	$\bar{K}N$	1.78	$-1.76-0.24i$	**0.795**	(**0.597**)
						$\eta\Lambda$	0.94	$-0.94-0.06i$	0.023	(0.040)
						$K\Xi$	0.10	$0.05+0.09i$	0.000	(0.000)
						$\bar{K}^*N$	2.18	$2.18+0.06i$	**0.066**	(**0.126**)
						$\omega\Lambda$	0.48	$0.48+0.06i$	0.003	(0.004)
						$\rho\Sigma$	0.34	$0.18-0.29i$	−0.001	(−0.003)
						$\phi\Lambda$	0.88	$0.88+0.05i$	0.007	(0.013)
						$\rho\Sigma^*$	0.40	$0.39-0.09i$	0.002	(0.002)
						$K^*\Xi$	0.17	$0.03-0.17i$	0.000	(−0.001)
						$K^*\Xi^*$	0.06	$0.05-0.03i$	0.000	(0.000)
$\Lambda(1405)$	$\frac{1}{2}^-$	1	1373.0	170.0	0.332	$\pi\Sigma$	2.62	$2.07-1.60i$	**0.353**	(**0.586**)
		(1.12)	(1405.0)	(376.1)	(0.522)	$\bar{K}N$	1.03	$-0.78+0.67i$	−0.024	(−0.018)
						$\eta\Lambda$	0.21	$0.07+0.20i$	−0.001	(0.001)
						$K\Xi$	0.46	$0.29-0.36i$	−0.001	(−0.005)
						$\bar{K}^*N$	0.57	$-0.51+0.26i$	0.003	(0.004)
						$\omega\Lambda$	0.24	$-0.02-0.24i$	−0.001	(0.002)
						$\rho\Sigma$	1.68	$-1.37+0.97i$	0.006	(−0.023)
						$\phi\Lambda$	0.17	$-0.07-0.16i$	0.000	(0.000)
						$\rho\Sigma^*$	0.66	$-0.45+0.48i$	−0.001	(−0.011)
						$K^*\Xi$	0.93	$-0.63+0.69i$	−0.002	(−0.011)
						$K^*\Xi^*$	0.29	$0.01+0.29i$	−0.001	(−0.003)
$\Lambda(1520)$	$\frac{3}{2}^-$	1	1540.0	74.0	0.274	$\pi\Sigma^*$	2.29	$2.03-1.05i$	**0.227**	(**0.109**)
		(0.780)	(1522.7)	(25.9)	(0.134)	$\bar{K}^*N$	0.87	$0.84-0.23i$	0.011	(0.005)
						$\omega\Lambda$	0.40	$-0.31+0.26i$	0.000	(0.001)
						$\rho\Sigma$	1.18	$1.09-0.46i$	0.015	(0.008)
						$K\Xi^*$	0.63	$0.49-0.40i$	0.001	(0.001)
						$\phi\Lambda$	0.04	$0.02-0.03i$	0.000	(0.000)
						$\rho\Sigma^*$	1.60	$1.42-0.74i$	0.015	(0.009)
						$K^*\Xi$	0.55	$-0.50+0.24i$	0.002	(0.001)
						$K^*\Xi^*$	0.59	$0.46-0.37i$	0.001	(0.000)

with their couplings, g_i, to the different meson-baryon channels are shown in Tables III, IV and V. In the case we want to refer to a specific flavor we will write Λ_s, Λ_c or Λ_b. For each flavor $f = s, c, b$, the resonances Λ_f are ordered by closeness to the $\pi\Sigma_f$ threshold, and they are displayed in this sequence in the Tables.

We use the convoluted meson-baryon propagator for the nonstable intermediate particles (namely, ρ, K^* and $\bar{K}^*$ mesons and Σ^* baryon) in the study of the strange sector for the $\Lambda(1405)$ and $\Lambda(1520)$ resonances, in a similar manner as done in Ref. [62]. In Ref. [33], it was reported that the convolution did not affect the dynamically generated Λ_c states in a substantial manner as the dominant convoluted meson-baryon channels were far from the position of the heavy Λ_c states.

In view of their mass position and dominant couplings, we assign these states to the experimental strange [$\Lambda(1405)$, $\Lambda(1520)$], charmed [$\Lambda_c(2595$, $\Lambda_c(2625)$] and beauty [$\Lambda_b(5912)$, $\Lambda_b(5920)$] states, similarly to Refs. [31,33,34,62]. Note, however, that in Refs. [31,34] the subtraction point was slightly modified in order to fix the position of the dynamically generated states to the experimental predictions of the $\Lambda_c(2595)$ and $\Lambda_b(5912)$, respectively.

Three Λ states are obtained in each of the flavor sectors, two of them with $J^P = 1/2^-$ and one with $J^P = 3/2^-$. The well-known two-pole pattern of the $\Lambda(1405)$ [78,81,82] is reproduced for the $\Lambda_c(2595)$ and $\Lambda_b(5912)$. Indeed, for $J^P = 1/2^-$ we find a state that strongly couples to NM and NM^* channels, with $(M, M^*) = (\bar{K}, \bar{K}^*)$, (D, D^*) or $(\bar{B}, \bar{B}^*)$ for strange, charm or beauty sectors, respectively. The $\bar{K}N$ dominance in the $\Lambda(1405)$ has gotten some support from lattice QCD calculations [83]. In addition, a second state $1/2^-$ coupling to $B\pi$, with $B = \Sigma, \Sigma_c$ or Σ_b is

TABLE IV. Same as Table III for the charm sector.

State	J^P	$\sqrt{\alpha}$	M_R	Γ_R	$1-Z$	Channel	$\lvert g_i\rvert$	g_i	X_i	(X_i')
$\Lambda_c(2595)$	$\frac{1}{2}^-$	1	2619.0	1.2	0.878	$\pi\Sigma_c$	0.31	$0.22+0.22i$	-0.012	(-0.023)
		(0.979)	(2592.3)	(0.3)	(0.844)	DN	3.49	$-3.49-0.14i$	**0.275**	(**0.292**)
						$\eta\Lambda_c$	0.40	$0.40+0.00i$	0.007	(0.009)
						D^*N	5.64	$-5.64+0.14i$	**0.465**	(**0.451**)
						$K\Xi_c$	0.22	$0.22+0.00i$	0.002	(0.001)
						$\omega\Lambda_c$	0.18	$0.18+0.04i$	0.001	(0.001)
						$K\Xi_c'$	0.04	$0.02+0.04i$	0.000	(0.000)
						$D_s\Lambda$	1.38	$-1.38+0.01i$	0.026	(0.026)
						$D_s^*\Lambda$	2.87	$-2.87+0.03i$	**0.086**	(**0.057**)
						$\rho\Sigma_c$	0.41	$0.39+0.12i$	0.003	(0.005)
						$\eta'\Lambda_c$	0.92	$0.92+0.01i$	0.018	(0.018)
						$\rho\Sigma_c^*$	0.58	$0.58-0.07i$	0.007	(0.006)
						$\phi\Lambda_c$	0.01	$0.01+0.00i$	0.000	(0.000)
						$K^*\Xi_c$	0.05	$0.02+0.05i$	0.000	(0.000)
						$K^*\Xi_c'$	0.16	$0.16+0.04i$	0.000	(0.000)
						$K^*\Xi_c^*$	0.15	$0.15+0.02i$	0.000	(0.000)
$\Lambda_c(2595)$	$\frac{1}{2}^-$	1	2617.0	90.0	0.401	$\pi\Sigma_c$	2.36	$2.09-1.09i$	**0.325**	(**0.252**)
		(0.950)	(2595.0)	(36.8)	(0.354)	DN	1.64	$-1.46+0.75i$	0.027	(0.015)
						$\eta\Lambda_c$	0.06	$0.02-0.06i$	0.000	(0.000)
						D^*N	1.43	$1.34+0.51i$	0.024	(**0.057**)
						$K\Xi_c$	0.04	$0.02-0.03i$	0.000	(0.000)
						$\omega\Lambda_c$	0.43	$0.30-0.31i$	0.000	(0.003)
						$K\Xi_c'$	0.48	$0.38-0.29i$	0.001	(0.002)
						$D_s\Lambda$	0.21	$0.07+0.20i$	0.000	(0.001)
						$D_s^*\Lambda$	0.40	$0.22+0.33i$	-0.001	(0.002)
						$\rho\Sigma_c$	1.28	$1.11-0.63i$	0.016	(0.013)
						$\eta'\Lambda_c$	0.13	$-0.07-0.11i$	0.000	(0.001)
						$\rho\Sigma_c^*$	0.70	$-0.64+0.28i$	0.006	(0.006)
						$\phi\Lambda_c$	0.01	$0.01+0.01i$	0.000	(0.000)
						$K^*\Xi_c$	0.51	$0.45-0.25i$	0.002	(0.002)
						$K^*\Xi_c'$	0.29	$0.10-0.27i$	0.000	(0.001)
						$K^*\Xi_c^*$	0.20	$-0.15+0.13i$	0.000	(0.000)
$\Lambda_c(2625)$	$\frac{3}{2}^-$	1	2667.0	55.0	0.365	$\pi\Sigma_c^*$	2.19	$1.97-0.95i$	**0.268**	(**0.319**)
		(0.807)	(2628.1)	(0.0)	(0.405)	D^*N	2.03	$1.96-0.51i$	**0.057**	(**0.044**)
						$\omega\Lambda_c$	0.53	$-0.45+0.28i$	0.003	(0.018)
						$K\Xi_c^*$	0.42	$0.34-0.24i$	0.002	(0.001)
						$D_s^*\Lambda$	0.06	$0.05-0.04i$	0.000	(0.000)
						$\rho\Sigma_c$	0.75	$0.68-0.31i$	0.008	(0.005)
						$\rho\Sigma_c^*$	1.30	$1.17-0.57i$	0.022	(0.013)
						$\phi\Lambda_c$	0.01	$-0.01+0.01i$	0.000	(0.000)
						$K^*\Xi_c$	0.61	$-0.55+0.27i$	0.005	(0.004)
						$K^*\Xi_c'$	0.25	$0.22-0.12i$	0.001	(0.000)
						$K^*\Xi_c^*$	0.40	$0.33-0.23i$	0.001	(0.001)

also seen for strangeness, charm or beauty, respectively. (In what follows we simply refer to these two $\Lambda(\frac{1}{2}^-)$ states as "first" and "second" state, respectively). On the other hand, the $J^P = 3/2^-$ states $\Lambda_c(2625)$ and $\Lambda_b(5920)$ are the counterparts in the charm and beauty sectors of the $\Lambda(1520)$.

In Refs. [31,33,34,62], the *coupling constants* were interpreted as a measure of the importance of a channel in order to determine the molecular nature of the state. For instance, the $\Lambda(1405)$ state close to the scattering line would be a mixture of $\bar{K}N$ and $\bar{K}^*N$ states, while the second $\Lambda(1405)$ state, with a very large decay width, would be mainly a $\pi\Sigma$ state. In the next section, we argue that the coupling constants, though useful, are not sufficient to describe the nature of a resonance. Thus, further analyses of the nature and, hence, of the *compositeness* of the Λ states are required.

III. COMPOSITENESS OF THE Λ STATES

In Ref. [43] Weinberg analyzed the nature of the deuteron and found that this particle is best described as

TABLE V. Same as Table III for the beauty sector.

State	J^P	$\sqrt{\alpha}$	M_R	Γ_R	$1-Z$	Channel	g_i	X_i	(X_i')
$\Lambda_b(5912)$	$\frac{1}{2}^-$	1	5878.0	0.0	0.956	$\pi\Sigma_b$	0.04	0.000	(0.000)
		(1.01)	(5912.1)	(0.0)	(0.958)	$\bar{B}N$	−4.55	**0.205**	(**0.217**)
						$\eta\Lambda_b$	0.33	0.006	(0.010)
						$\bar{B}^*N$	−7.70	**0.539**	(**0.561**)
						$K\Xi_b$	0.22	0.002	(0.002)
						$\omega\Lambda_b$	0.04	0.000	(0.000)
						$K\Xi_b'$	0.02	0.000	(0.000)
						$\bar{B}_s\Lambda$	−1.96	0.031	(0.031)
						$\bar{B}_s^*\Lambda$	−4.01	**0.122**	(**0.084**)
						$\rho\Sigma_b$	0.38	0.005	(0.006)
						$\eta'\Lambda_b$	0.96	0.032	(0.032)
						$\rho\Sigma_b^*$	0.57	0.011	(0.013)
						$\phi\Lambda_b$	0.02	0.000	(0.000)
						$K^*\Xi_b$	−0.01	0.000	(0.000)
						$K^*\Xi_b'$	0.17	0.001	(0.000)
						$K^*\Xi_b^*$	0.19	0.001	(0.001)
$\Lambda_b(5912)$	$\frac{1}{2}^-$	1	5949.0	0.0	0.865	$\pi\Sigma_b$	1.31	**0.698**	(**0.397**)
		(0.984)	(5912.0)	(0.0)	(0.788)	$\bar{B}N$	−2.90	**0.096**	(**0.215**)
						$\eta\Lambda_b$	0.01	0.000	(0.000)
						$\bar{B}^*N$	1.91	0.038	(**0.082**)
						$K\Xi_b$	−0.01	0.000	(0.000)
						$\omega\Lambda_b$	0.78	0.028	(**0.088**)
						$K\Xi_b'$	0.18	0.001	(0.001)
						$\bar{B}_s\Lambda$	−0.01	0.000	(0.000)
						$\bar{B}_s^*\Lambda$	0.18	0.000	(0.000)
						$\rho\Sigma_b$	0.13	0.001	(0.002)
						$\eta'\Lambda_b$	−0.03	0.000	(0.000)
						$\rho\Sigma_b^*$	−0.08	0.000	(0.001)
						$\phi\Lambda_b$	0.00	0.000	(0.000)
						$K^*\Xi_b$	0.23	0.002	(0.002)
						$K^*\Xi_b'$	0.13	0.001	(0.000)
						$K^*\Xi_b^*$	−0.10	0.000	(0.000)
$\Lambda_b(5920)$	$\frac{3}{2}^-$	1	5963.0	0.0	0.818	$\pi\Sigma_b^*$	1.54	**0.581**	(**0.356**)
		(0.983)	(5919.7)	(0.0)	(0.785)	$\bar{B}^*N$	4.16	**0.185**	(**0.319**)
						$\omega\Lambda_b$	−0.99	0.046	(**0.102**)
						$K\Xi_b^*$	0.20	0.002	(0.001)
						$\bar{B}_s^*\Lambda$	0.14	0.000	(0.000)
						$\rho\Sigma_b$	0.08	0.000	(0.001)
						$\rho\Sigma_b^*$	0.12	0.001	(0.005)
						$\phi\Lambda_b$	0.00	0.000	(0.000)
						$K^*\Xi_b$	−0.28	0.003	(0.002)
						$K^*\Xi_b'$	0.08	0.000	(0.000)
						$K^*\Xi_b^*$	0.17	0.001	(0.000)

composed of a proton and a neutron, rather than a genuine dibaryon. More recently, the issue of compositeness was addressed in Ref. [44–46] for s-waves and small binding energies. An extension to larger binding energies in coupled-channels dynamics was undertaken in Ref. [47] for bound states and in Refs. [48–51] for resonances. In this section we summarize the formalism and the conclusions derived in Ref. [51] for the interpretation of the Weinberg's sum rule and its generalization to resonances.

In the unitarized setting the sum rule follows from the identity [52,56,57,84]:

$$-1 = \sum_{i,j} g_i g_j \left(\delta_{ij} \frac{\partial G_i(\sqrt{s})}{\partial \sqrt{s}} + G_i(\sqrt{s}) \frac{\partial V_{ij}(\sqrt{s})}{\partial \sqrt{s}} G_j(\sqrt{s}) \right) \Bigg|_{\sqrt{s}=\sqrt{s_R}}. \quad (9)$$

This relation is derived in Appendix B. It holds for bounds states and resonances, as well as energy dependent or energy independent interactions.

The use of the definitions

$$X_i = -\mathrm{Re}\left(g_i^2 \frac{dG_i}{d\sqrt{s}}\bigg|_{\sqrt{s_R}} \right),$$
$$Z = -\mathrm{Re}\sum_{i.j} g_i g_j \left(G_i \frac{\partial V_{ij}}{\partial \sqrt{s}} G_j \right)\bigg|_{\sqrt{s_R}} \qquad (10)$$

provides the sum rule

$$1 = Z + \sum_i X_i. \qquad (11)$$

For bound states the extraction of the real part in Eq. (10) is redundant since the quantities involved are already real. The expression of X_i involves the derivative of the loop function. The analytical expression of this function on the first and second Riemann sheets is made explicit in Appendix A.

As follows from the analysis in [51], for bound states, the quantity X_i is related to the probability of finding the state in the channel i. For resonances, X_i is still related to the squared wave function of the channel i, in a phase prescription that automatically renders the wave function real for bound states, and so it can be used as a measure of the weight of that meson-baryon channel in the composition of the resonant state.

The quantity $\sum_i X_i = 1 - Z$ represents the *compositeness* of the hadronic state in terms of all the considered channels, and Z is referred to as its *elementariness*. A nonvanishing Z takes into account that ultimately the model is an effective one. The energy dependent interaction effectively accounts for other possible interaction mechanisms not explicitly included in the s-wave meson-baryon description. These could be other hadron-hadron interactions, or even genuine negative-parity baryonic components not of the molecular type (hence the appellative elementariness). Thus, a small value of Z indicates that the state is well described by the contributions explicitly considered, namely, s-wave meson-baryon channels. Conversely, a large value of Z indicates that, for that state, significant pieces of information are missing in the model, and this information is being included through an effective interaction, to the extent that the experimental hadronic properties are reproduced by the model.

The results we obtain for the compositeness weights, X_i, and aggregated compositeness $1 - Z$ of the various Λ states are displayed in Tables III, IV and V, for the default value $\alpha = 1$ and also for another phenomenological choice of the subtraction point, so that the experimental masses are better reproduced. As mentioned in the introduction, the results reported in Refs. [56,57] are in qualitative agreement with those presented in Table III for the $\Lambda(1405)$ states. In what follows we draw some conclusions with regards to the nature of the Λ states and its variation with the quark mass that can be extracted from the numbers.

First, the contribution of each meson-baryon channel to the dynamical generation of a state is determined not only by the value of the coupling constant but also depends on the closeness of meson-baryon channel to the state. For instance, the $\bar{K}N$ and $\bar{K}^*N$ channels have similar couplings to the first pole of $\Lambda(1405)$ but their contribution to the compositeness is quite different due to their different thresholds, relative to the mass of the state.

Second, the neglected contributions can be measured by means of the elementariness. Indeed, we observe that those Λ poles close to the scattering line are well described as molecular states through the s-wave meson-baryon channels considered, while wider states need the consideration of other contributions, such as multihadron scattering. This is clearly manifest for the $J^P = 3/2^-$ states $\Lambda(1520)$ and $\Lambda_c(2625)$. There is, however, not a strict correlation between the value of the width and the elementariness. The $1/2^-$ states have a larger compositeness than their $3/2^-$ counterparts.

Third, taking the natural identification between different Λ states for different flavors, one observes that as a rule, the heavier the flavor the larger the compositeness of the resonance. For instance, the $\Lambda(1520)$, $\Lambda_c(2625)$ and $\Lambda_b(5920)$ states have $1 - Z = 0.27$, 0.37, and 0.82, respectively (for $\alpha = 1$).

In the tables we primarily display results for the default value $\alpha = 1$, even though this choice of subtraction point does not reproduce the empirical masses of the resonances in detail. We also display results with α suitably fitted in each case so that empirical masses of the resonances are reproduced. For the sake of definiteness, an equal mass for the two $1/2^-$ Λ states of each flavor has been adopted. The purpose of doing this is not to achieve a precise description of the resonance, but rather to see to what extent the subtraction point and the resonance position are relevant for the compositeness discussion. We can see that no substantial modifications in the weights X_i take place in the charm and beauty cases, and the same holds for the first $\Lambda(1405)$ state. The change is somewhat larger for the second $\Lambda(1405)$ state and for the $\Lambda(1520)$ resonance. For these two resonances, the change required in the subtraction points is also sizable.

In order to understand these features, one can observe that the three first Λ states, namely, $\Lambda(1405)$, $\Lambda_c(2595)$ and $\Lambda_b(5912)$, have sizable weights (X_i) in the nucleon-pseudoscalar channel, $\bar{K}N$, DN and $\bar{B}N$, respectively, while the weights of the Σ-pseudoscalar lightest channels, $\pi\Sigma$, $\pi\Sigma_c$ and $\pi\Sigma_b$, are much smaller or even negligible in the bottom case. The couplings (g_i) to these two types of channels follow a similar trend, and this explains the small widths of these resonances. In fact, for the $\Lambda(1405)$, the

$\bar{K}N$ channel is dominant as regards to compositeness (although the coupling to $\bar{K}^*N$ is also large). For the $\Lambda_c(2595)$ and $\Lambda_b(5912)$, the weight of DN and $\bar{B}N$ is important but competes with D^*N and $\bar{B}^*N$. For the charm (bottom) sector this was also found in [31,33] ([34]) and in [25]. Likely, this is a consequence of the similar roles played by vector and pseudoscalar heavy mesons (D and D^* or $\bar{B}$ and $\bar{B}^*$) due to heavy quark symmetry. The fact that these first $\Lambda(1405)$, $\Lambda_c(2595)$ and $\Lambda_b(5912)$ poles have compositeness $1-Z$ close to unity indicates that the present model, with s-wave meson-baryon including pseudoscalar and vector mesons, gives a fair description of these resonances.

Likewise, the compositeness is large in the case of the second $\Lambda_b(5912)$ and the $\Lambda_b(5920)$, suggesting that the model is also fairly complete for these two resonances.

Small values of $1-Z$, below 0.5, are found for the second $\Lambda(1405)$ and the second $\Lambda_c(2595)$ in the $1/2^-$ sector, as well as the $\Lambda(1520)$ and $\Lambda_c(2625)$ in the $3/2^-$ sector. A conspicuous difference between the first and second $\Lambda(1/2^-)$ resonances is that the latter states strongly couple to the lightest channel $\pi\Sigma$ or $\pi\Sigma_c$, and this channel largely saturate their compositeness $1-Z$. The same applies to the $3/2^-$ Λ states, this time with $\pi\Sigma^*$ or $\pi\Sigma_c^*$ channels. As a consequence, these four resonances have a sizable width. Related to this, the available phase-space of the meson-baryon pair allows mechanisms involving higher partial waves (beyond s-wave) to play a role in the composition of the resonance. These missing mechanisms would be accounted for by the larger values of Z displayed by these four resonances.

Within the molecular approach, the first missing interaction mechanism is expected to come from d-wave interactions. These type of interactions have been considered in Ref. [55] for the $\Lambda(1520)$. The specific channels considered there are $\pi\Sigma^*$ and $K\Xi^*$ in s-wave, and $\bar{K}N$ and $\pi\Sigma$ in d-wave. Further, the interaction is modeled as to reproduce $\bar{K}N$ scattering data, and several fits consistent with the experimental mass of the $\Lambda(1520)$ are presented. That calculation suggests that d-wave components play an important role in the structure of the $\Lambda(1520)$. In Fig. 1 we display a comparison between our results and those in [55] for the weights of each channel. The vertical lines interpolate between the different values given in that work for different fits. While we have not included higher partial waves in our interaction, we find that the weights of the s-wave channels included in [55] are qualitatively similar in both calculations and the agreement improves as the position of the pole is moved to its experimental value by a change of subtraction point. It can also be seen that other s-wave channels are more relevant than $K\Xi^*$, namely, $\bar{K}^*N$, $\rho\Sigma$ and $\rho\Sigma^*$, although $\pi\Sigma^*$ is the dominant one in our model.

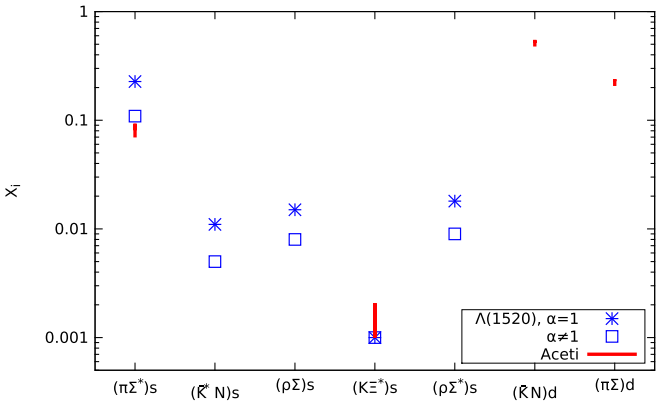

FIG. 1 (color online). Weights X_i of the main channels contributing to the composition of the $\Lambda(1520)$. Our results (in blue) are represented by stars for $\alpha = 1$, and by squares when the subtraction point is modified to bring the mass of the resonance to its experimental value. The vertical lines (in red) indicate the weights obtained in [55] for the two s-wave and two d-wave channels considered there using various sets of fitting parameters.

IV. SUMMARY AND CONCLUSIONS

In this work we have studied the nature of the lowest-lying negative-parity Λ resonances with strange, charm or bottom flavors, with $J^P = \frac{1}{2}^-$ and $\frac{3}{2}^-$. To this end we have adopted a description based on pseudoscalar and vector mesons interacting in s-wave with $\frac{1}{2}^+$ and $\frac{3}{2}^+$ baryons. The model, spelled out in [35], is based on spin-flavor and heavy-quark extensions of the WT interaction, thereby embodying the correct symmetries in the appropriate limits, such as chiral symmetry and HQSS. (The symmetries are explicitly broken at the level of masses and decay constants of the basic hadrons.) The interaction is then used as an input of the Bethe-Salpeter equation in coupled-channels. The model has no free parameters, barring the choice of subtraction point in the renormalization of the loop function. This is fixed by a prescription, or occasionally used to modify the positions of the resonances to fulfill phenomenological constraints.

As already uncovered by previous studies, we find a double pole structure for the states with $J^P = \frac{1}{2}^-$ and a single pole for the states with $\frac{3}{2}^-$ for each of the three flavors. The novelty comes from the systematic study of the composition of these resonances, as a function of the heavy quark mass, addressing the question of to what extent the structure of the resonances is fully saturated by the available s-wave meson-baryon channels.

Regarding the overall compositeness of the nine Λ resonances studied, we find that for a given flavor sector, the closer to threshold (on the complex plane) the better the resonance is described as an s-wave meson-baryon molecule. Also, the heavier the flavor the higher the compositeness $1-Z$. More explicitly, we find that $1-Z$ is large for the first $\Lambda(\frac{1}{2}^-)$ of each flavor and the compositeness

decreases as we move to the second $\Lambda(\frac{1}{2}^-)$ states and then to the $\Lambda(\frac{3}{2}^-)$ ones. Also, the compositeness is large for all bottom Λ states. This would indicate that the three first $\Lambda(\frac{1}{2}^-)$ and all the rest of the bottom resonances considered are largely saturated, regarding their composition, by s-wave meson-baryon channels. This would not be so for the strange and charmed second $\Lambda(\frac{1}{2}^-)$ and strange and charmed $\Lambda(\frac{3}{2}^-)$ resonances, which would require further components to achieve the saturation of the sum rule.

With respect to the detailed composition of the states, we find that the first $\Lambda(\frac{1}{2}^-)$ states of each flavor couple strongly to pseudoscalar-N and vector-N channels. This is a manifestation of spin-flavor symmetry between pseudoscalar and vector partners, and in particular HQSS in the charm and bottom cases. For the $\Lambda(1405)$ this implies that the pseudoscalar-N channel, being lighter than the vector-N one, almost saturates the compositeness of the state. It is noteworthy that a large weight of $\bar{K}N$ in the $\Lambda(1405)$ has been recently reported from lattice QCD calculations [83]. The situation changes for charm and bottom flavors where the two channels (DN and D^*N or $\bar{B}N$ and $\bar{B}^*N$) are relatively closer due to HQSS. In this case, the weights of the channels follows more closely the trend of the couplings. (Although with smaller weights, a similar pattern appears for the strange partners of the mesons, $D_s\Lambda$, $D_s^*\Lambda$, etc., due to SU(3)-light flavor symmetry.) These two channels almost saturate the composition of the first $\Lambda_c(2595)$ and $\Lambda_b(5912)$ states.

For the second $\Lambda(\frac{1}{2}^-)$ states, the main observation is its sizable coupling to the lightest channels $\pi\Sigma$, $\pi\Sigma_c$ and $\pi\Sigma_b$. As a consequence these states are effectively more excited than the first $\Lambda(\frac{1}{2}^-)$ states and for the strange and charm flavor this explains their larger widths, as compared to the first states. The larger phase space also implies that higher partial waves could play a role, consistently with the fact that they are much less saturated by the s-wave meson-baryon channels considered here.

Another observation is the similar structure of the second $\Lambda(\frac{1}{2}^-)$ and $\Lambda(\frac{3}{2}^-)$ states, which appear as HQSS or spin-flavor partners. This is particularly clear in the bottom case, where HQSS works better. The couplings of $\pi\Sigma_b$ in the second $\Lambda_b(5912)$ and $\pi\Sigma_b^*$ in $\Lambda_b(5920)$ are similar and, the same pattern is seen for $\bar{B}N$ and $\bar{B}^*N$. This translates to the corresponding composition weights, although distorted by the effect of different excitation energy of the channels. The spin-flavor symmetry between Σ_c and Σ_c^*, and Σ and Σ^* still acts for charm and strange flavors.

Although beyond the scope of the present work, it would be interesting to consider also quark models and try to compare to hadronic results in order to see whether the composition of a given resonance can be termed as molecular, made of quarks or hybrid, and if possible to quantify the hybrid mixture.

ACKNOWLEDGMENTS

We thank E. Oset for careful proofreading and comments. C. H.-D. thanks the support of the JAE-CSIC Program. This research was supported by Spanish Ministerio de Economía y Competitividad and European FEDER funds under Contracts No. FPA2010-16963, No. FIS2011-28853-C02-02, No. FPA2013-43425-P, No. FIS2014-59386-P, No. FIS2014-51948-C2-1-P and No. FIS2014-57026-REDT, and by Junta de Andalucía, Grant No. FQM-225. L. T. acknowledges support from the Ramón y Cajal Research Programme from Ministerio de Ciencia e Innovación and from FP7-PEOPLE-2011-CIG under Contract No. PCIG09-GA-2011-291679.

APPENDIX A: DERIVATIVE OF THE LOOP FUNCTION

In order to compute analytically the derivative of the (s-wave) loop function required in Eq. (10), we recall its definition in Eq. (3):

$$G = i2M \int \frac{d^4q}{(2\pi)^4} \frac{1}{q^2 - m^2 + i\epsilon} \frac{1}{(P-q)^2 - M^2 + i\epsilon}, \quad M, m > 0. \tag{A1}$$

Choosing the CM frame, $P^\mu = (\sqrt{s}, \mathbf{0})$, its partial derivative with respect to the energy can be written as

$$G'(\sqrt{s}) \equiv \frac{\partial G}{\partial \sqrt{s}} = -i4M \int \frac{d^4q}{(2\pi)^4} \frac{1}{q^2 - m^2 + i\epsilon} \times \frac{P^0 - q^0}{((P-q)^2 - M^2 + i\epsilon)^2}. \tag{A2}$$

Unlike the loop function, $G'(\sqrt{s})$ is ultraviolet convergent. The use of a standard Feynman's parametrization (see e.g. Eq. (10.13) of [85]) gives

$$G' = -i8M \int \frac{d^4q}{(2\pi)^4} \int_0^1 dx \frac{x(P^0 - q^0)}{[(q - xP)^2 - x^2P^2 - m^2 + (P^2 - M^2 + m^2)x + i\epsilon]^3}, \tag{A3}$$

and after a translation in the integration variable:

$$G' = -i8M\sqrt{s} \int_0^1 dx \int \frac{d^4q}{(2\pi)^4} \frac{x(1-x)}{(q^2 + x(1-x)s - (1-x)m^2 - xM^2 + i\epsilon)^3}. \tag{A4}$$

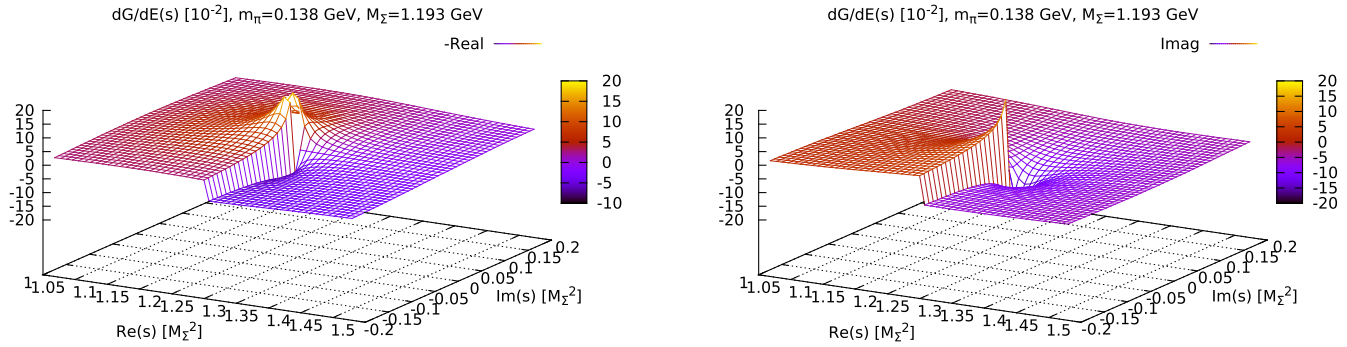

FIG. 2 (color online). Function $G'(\sqrt{s})$. On the left $-\mathrm{Re}G'$. On the right $+\mathrm{Im}G'$. The display corresponds to $m = m_\pi$ and $M = M_\Sigma$.

The integral over the q^μ is now straightforward (using e.g. Eq. (A.44) of [86]) to obtain

$$G' = \frac{M\sqrt{s}}{4\pi^2}\int_0^1 dx \frac{1}{s - \frac{m^2}{x} - \frac{M^2}{1-x} + i\epsilon}. \tag{A5}$$

It follows that G' is purely real for $s < (M+m)^2$, while $\mathrm{Im}G' < 0$ for $s > (M+m)^2$.

The integral Eq. (A5) is well defined for $\sqrt{s}$ on the complex plane, excluding $s = (M+m)^2$, and it yields

$$G' = \frac{M}{4\pi^2 s\sqrt{s}}\left(s - (M^2 - m^2)\log\frac{M}{m} - \frac{s(M^2+m^2) - (M^2-m^2)^2}{\sqrt{s-s_+}\sqrt{s-s_-}}\log\frac{\sqrt{s-s_+} - \sqrt{s-s_-}}{\sqrt{s-s_+} + \sqrt{s-s_-}}\right) \tag{A6}$$

with

$$s_\pm = (M \pm m)^2, \qquad \mathrm{Arg}\sqrt{s-s_+} \in [0,\pi), \qquad \mathrm{Arg}\sqrt{s-s_-} \in \left[-\frac{\pi}{2}, \frac{\pi}{2}\right), \qquad \mathrm{Im}\log \in [0,\pi] \quad \text{(FRS)}. \tag{A7}$$

The function $G'(\sqrt{s})$ inherits the branching points and Riemann sheet structure of the loop function G. The expression in Eqs. (A6) and (A7) corresponds to the so-called first Riemann sheet (FRS) with respect to the s_+ branching point and the branch cut is along $s \geq s_+$. For the FRS, the point $s = s_-$ is a regular point. s_+ is a branching point of order one (by circling twice around s_+ the function returns to its original value) hence there is a second Riemann sheet (SRS) with respect to s_+ that continues the FRS at the two borders of the selected cut. The SRS is obtained by analytic continuation. The point $s = s_-$ is a branching point of order one in the SRS. However, for the physical phase space of interest the new Riemann sheets introduced by the branching at s_- are not relevant. The expression of $G'(\sqrt{s})$ on the SRS takes the same form as in Eq. (A6) but taking

$$\mathrm{Arg}\sqrt{s-s_+} \in [0,\pi), \qquad \mathrm{Arg}\sqrt{s-s_-} \in \left[\frac{\pi}{2}, \frac{3\pi}{2}\right), \qquad \mathrm{Im}\log \in [\pi, 2\pi] \quad \text{(SRS)}. \tag{A8}$$

The function $G'(\sqrt{s})$ is displayed in Fig. 2. In the plot $\sqrt{s}$ is on the FRS when $\mathrm{Re}(s) < (M+m)^2$ or when $\mathrm{Re}(s) > (M+m)^2$ and $\mathrm{Im}(s) > 0$, and on the SRS when $\mathrm{Re}(s) > (M+m)^2$ and $\mathrm{Im}(s) < 0$. The bound states fall on the "negative" (with respect to $M+m$) real axis and the resonances fall below the "positive" real axis, for the relevant channel. This cut of the complex plane covers most cases. An exception is the $\Lambda(1520)$ with $\sqrt{\alpha} = 0.780$, which falls slightly at the left of the branch cut, for $\pi\Sigma^*$.

For completeness we give here the analytical form of the loop function, subtracted at $s = s_+$:

$$G = -\frac{M}{8\pi^2 s}\left((s-s_+)\frac{M-m}{M+m}\log\frac{M}{m} + \sqrt{s-s_+}\sqrt{s-s_-}\log\frac{\sqrt{s-s_+} - \sqrt{s-s_-}}{\sqrt{s-s_+} + \sqrt{s-s_-}}\right). \tag{A9}$$

The choices of branches for the FRS and the SRS are as in Eqs. (A7) and (A8), respectively.

APPENDIX B: COMPOSITENESS SUM RULE

In this appendix we prove the relation in Eq. (9). We start from Eq. (2)

$$T(\sqrt{s}) = (V^{-1}(\sqrt{s}) - G(\sqrt{s}))^{-1} \tag{B1}$$

where T, V and G are matrices and G is diagonal. Taking a derivative with respect to $\sqrt{s}$ [using the operator identity $\delta(A^{-1}) = -A^{-1}\delta A A^{-1}$]

$$T' = T(G' + V^{-1}V'V^{-1})T. \tag{B2}$$

On the other hand, Eq. (8) implies

$$T_{ij} = \frac{g_i g_j}{\Delta} + R_{ij}(\sqrt{s}), \qquad \Delta \equiv \sqrt{s} - \sqrt{s_R}, \tag{B3}$$

where the remainder R_{ij} is regular at the pole. Taking a derivative with respect to Δ, substituting T in Eq. (B2) and multiplying by Δ^2 gives, at $\Delta = 0$,

$$-g_i g_j = \sum_{k,l} g_i g_k \left(G'_k \delta_{kl} + \sum_{r,s} (V^{-1})_{kr} V'_{rs} (V^{-1})_{sl} \right)_{\Delta=0} g_l g_j. \tag{B4}$$

Since at least one of the couplings must be different from zero (to have a pole) it follows that

$$-1 = \sum_{k,l} g_k g_l \left(G'_k \delta_{kl} + \sum_{r,s} (V^{-1})_{kr} V'_{rs} (V^{-1})_{sl} \right)\Big|_{\Delta=0}. \tag{B5}$$

To arrive to Eq. (9) it only remains to show that $(V^{-1})_{sl}$ can be replaced by $\delta_{sl} G_l$ in Eq. (B5). This follows from $V^{-1} = T^{-1} + G$ and $\sum_l (T^{-1})_{jl} g_l|_{\Delta=0} = 0$. The latter equality can be deduced from,

$$\sum_l (T^{-1})_{jl} \left(\frac{g_l g_j}{\Delta} + R_{lj}(\sqrt{s}) \right) = 1 \tag{B6}$$

without summing over the index j, which trivially follows from Eq. (B3) and $T^{-1}T = 1$. Thus, in the limit $\Delta \to 0$, we find

$$\lim_{\Delta\to 0} \sum_l (T^{-1})_{jl} g_l = \lim_{\Delta\to 0} \frac{\Delta}{g_j} = 0. \tag{B7}$$

The statement is trivial if there is just one channel. More generally, the singular part of T in Eq. (B3) is a matrix of rank one, the corresponding one-dimensional subspace being spanned by the vector g_i, in coupled-channels space. The combination $\sum_l (T^{-1})_{sl} g_l$ selects that subspace, in which T^{-1} vanishes at the pole.[3]

[3]The argument assumes that, at the pole, T is a regular matrix on the complementary subspace. For instance, it would not work for $T = \begin{pmatrix} \frac{g^2}{\Delta} & 1 \\ 1 & 0 \end{pmatrix}$, however, such a singular complement requires V to be singular at the resonance pole. We assume that this is not the case since V' would not exist at the pole.

[1] http://w4.lns.cornell.edu/Research/CLEO/.
[2] http://belle.kek.jp/.
[3] http://bes3.ihep.ac.cn/.
[4] http://www-public.slac.stanford.edu/babar/.
[5] http://www-panda.gsi.de/.
[6] http://j-parc.jp/index-e.html.
[7] R. Aaij *et al.* (LHCb Collaboration), Observation of Excited Λ_b^0 Baryons, Phys. Rev. Lett. **109**, 172003 (2012).
[8] L. Tolos, J. Schaffner-Bielich, and A. Mishra, Properties of D mesons in nuclear matter within a self-consistent coupled-channel approach, Phys. Rev. C **70**, 025203 (2004).
[9] L. Tolos, J. Schaffner-Bielich, and H. Stoecker, D-mesons: In-medium effects at FAIR, Phys. Lett. B **635**, 85 (2006).
[10] M. F. M. Lutz and E. E. Kolomeitsev, On charm baryon resonances and chiral symmetry, Nucl. Phys. **A730**, 110 (2004).
[11] M. F. M. Lutz and E. E. Kolomeitsev, Baryon resonances from chiral coupled-channel dynamics, Nucl. Phys. **A755**, 29 (2005).
[12] J. Hofmann and M. F. M. Lutz, Coupled-channel study of crypto-exotic baryons with charm, Nucl. Phys. **A763**, 90 (2005).
[13] J. Hofmann and M. F. M. Lutz, D wave baryon resonances with charm from coupled-channel dynamics, Nucl. Phys. **A776**, 17 (2006).
[14] M. F. M. Lutz and C. L. Korpa, Open-charm systems in cold nuclear matter, Phys. Lett. B **633**, 43 (2006).
[15] T. Mizutani and A. Ramos, D mesons in nuclear matter: A DN coupled-channel equations approach, Phys. Rev. C **74**, 065201 (2006).
[16] L. Tolos, A. Ramos, and T. Mizutani, Open charm in nuclear matter at finite temperature, Phys. Rev. C **77**, 015207 (2008).

[17] C. E. Jimenez-Tejero, A. Ramos, and I. Vidana, Dynamically generated open charmed baryons beyond the zero range approximation, Phys. Rev. C **80**, 055206 (2009).
[18] C. E. Jimenez-Tejero, A. Ramos, L. Tolos, and I. Vidana, Open charm meson in nuclear matter at finite temperature beyond the zero range approximation, Phys. Rev. C **84**, 015208 (2011).
[19] J. Haidenbauer, G. Krein, U. G. Meissner, and A. Sibirtsev, $\bar{N}$ interaction from meson-exchange and quark-gluon dynamics, Eur. Phys. J. A **33**, 107 (2007).
[20] J. Haidenbauer, G. Krein, U. G. Meissner, and A. Sibirtsev, Charmed meson rescattering in the reaction $\bar{p}d \downarrow \bar{D}DN$, Eur. Phys. J. A **37**, 55 (2008).
[21] J. Haidenbauer, G. Krein, U. G. Meissner, and L. Tolos, DN interaction from meson exchange, Eur. Phys. J. A **47**, 18 (2011).
[22] J.-J. Wu, R. Molina, E. Oset, and B. S. Zou, Prediction of Narrow N^* and Λ^* Resonances with Hidden Charm above 4 GeV, Phys. Rev. Lett. **105**, 232001 (2010).
[23] J.-J. Wu, R. Molina, E. Oset, and B. S. Zou, Dynamically generated N^* and Λ^* resonances in the hidden charm sector around 4.3 GeV, Phys. Rev. C **84**, 015202 (2011).
[24] E. Oset, A. Ramos, E. J. Garzon, R. Molina, L. Tolos, C. W. Xiao, J. J. Wu, and B. S. Zou, Interaction of vector mesons with baryons and nuclei, Int. J. Mod. Phys. E **21**, 1230011 (2012).
[25] W. H. Liang, T. Uchino, C. W. Xiao, and E. Oset, Baryon states with open charm in the extended local hidden gauge approach, Eur. Phys. J. A **51**, 16 (2015).
[26] W. H. Liang, C. W. Xiao, and E. Oset, Baryon states with open beauty in the extended local hidden gauge approach, Phys. Rev. D **89**, 054023 (2014).
[27] J.-J. Wu and B. S. Zou, Prediction of super-heavy N^* and Λ^* resonances with hidden beauty, Phys. Lett. B **709**, 70 (2012).
[28] N. Isgur and M. B. Wise, Weak decays of heavy mesons in the static quark approximation, Phys. Lett. B **232**, 113 (1989).
[29] M. Neubert, Heavy-quark symmetry, Phys. Rep. **245**, 259 (1994).
[30] A. V. Manohar and M. B. Wise, *Heavy Quark Physics*, Cambridge Monographs on Particle Physics, Nuclear Physics and Cosmology (Cambridge University Press, Cambridge, England, 2000), Vol. 10.
[31] C. Garcia-Recio, V. K. Magas, T. Mizutani, J. Nieves, A. Ramos, L. L. Salcedo, and L. Tolos, The s-wave charmed baryon resonances from a coupled-channel approach with heavy quark symmetry, Phys. Rev. D **79**, 054004 (2009).
[32] D. Gamermann, C. Garcia-Recio, J. Nieves, L. L. Salcedo, and L. Tolos, Exotic dynamically generated baryons with negative charm quantum number, Phys. Rev. D **81**, 094016 (2010).
[33] O. Romanets, L. Tolos, C. Garcia-Recio, J. Nieves, L. L. Salcedo, and R. G. E. Timmermans, Charmed and strange baryon resonances with heavy-quark spin symmetry, Phys. Rev. D **85**, 114032 (2012).
[34] C. Garcia-Recio, J. Nieves, O. Romanets, L. L. Salcedo, and L. Tolos, Odd parity bottom-flavored baryon resonances, Phys. Rev. D **87**, 034032 (2013).
[35] C. Garcia-Recio, J. Nieves, O. Romanets, L. L. Salcedo, and L. Tolos, Hidden charm N and Δ resonances with heavy-quark symmetry, Phys. Rev. D **87**, 074034 (2013).
[36] L. Tolos, Charming mesons with baryons and nuclei, Int. J. Mod. Phys. E **22**, 1330027 (2013).
[37] L. Tolos, C. Garcia-Recio, and J. Nieves, The properties of D and D^* mesons in the nuclear medium, Phys. Rev. C **80**, 065202 (2009).
[38] C. Garcia-Recio, J. Nieves, and L. Tolos, D mesic nuclei, Phys. Lett. B **690**, 369 (2010).
[39] C. Garcia-Recio, J. Nieves, L. L. Salcedo, and L. Tolos, D^- mesic atoms, Phys. Rev. C **85**, 025203 (2012).
[40] C. W. Xiao, J. Nieves, and E. Oset, Combining heavy quark spin and local hidden gauge symmetries in the dynamical generation of hidden charm baryons, Phys. Rev. D **88**, 056012 (2013).
[41] A. Ozpineci, C. W. Xiao, and E. Oset, Hidden beauty molecules within the local hidden gauge approach and heavy quark spin symmetry, Phys. Rev. D **88**, 034018 (2013).
[42] S. Weinberg, Elementary particle theory of composite particles, Phys. Rev. **130**, 776 (1963).
[43] S. Weinberg, Evidence that the deuteron is not an elementary particle, Phys. Rev. **137**, B672 (1965).
[44] C. Hanhart, Y. S. Kalashnikova, and A. V. Nefediev, Lineshapes for composite particles with unstable constituents, Phys. Rev. D **81**, 094028 (2010).
[45] V. Baru, J. Haidenbauer, C. Hanhart, Y. Kalashnikova, and A. E. Kudryavtsev, Evidence that the $a_0(980)$ and $f_0(980)$ are not elementary particles, Phys. Lett. B **586**, 53 (2004).
[46] M. Cleven, F. K. Guo, C. Hanhart, and U. G. Meissner, Bound state nature of the exotic Z_b states, Eur. Phys. J. A **47**, 120 (2011).
[47] D. Gamermann, J. Nieves, E. Oset, and E. Ruiz Arriola, Couplings in coupled channels versus wave functions: Application to the $X(3872)$ resonance, Phys. Rev. D **81**, 014029 (2010).
[48] J. Yamagata-Sekihara, J. Nieves, and E. Oset, Couplings in coupled channels versus wave functions in the case of resonances: Application to the two $\Lambda(1405)$ states, Phys. Rev. D **83**, 014003 (2011).
[49] F. Aceti and E. Oset, Wave functions of composite hadron states and relationship to couplings of scattering amplitudes for general partial waves, Phys. Rev. D **86**, 014012 (2012).
[50] C. W. Xiao, F. Aceti, and M. Bayar, The small $K\pi$ component in the K^* wave functions, Eur. Phys. J. A **49**, 22 (2013).
[51] F. Aceti, L. R. Dai, L. S. Geng, E. Oset, and Y. Zhang, Meson-baryon components in the states of the baryon decuplet, Eur. Phys. J. A **50**, 57 (2014).
[52] T. Hyodo, D. Jido, and A. Hosaka, Compositeness of dynamically generated states in a chiral unitary approach, Phys. Rev. C **85**, 015201 (2012).
[53] T. Hyodo, Structure of Near-Threshold s-Wave Resonances, Phys. Rev. Lett. **111**, 132002 (2013).
[54] H. Nagahiro and A. Hosaka, Elementarity of composite systems, Phys. Rev. C **90**, 065201 (2014).
[55] F. Aceti, E. Oset, and L. Roca, Composite nature of the $\Lambda(1520)$ resonance, Phys. Rev. C **90**, 025208 (2014).

[56] T. Sekihara and T. Hyodo, Size measurement of dynamically generated hadronic resonances with finite boxes, Phys. Rev. C **87**, 045202 (2013).

[57] T. Sekihara, T. Hyodo, and D. Jido, Comprehensive analysis of the wave function of a hadronic resonance and its compositeness, Prog. Theor. Exp. Phys. **2015**, 063D04 (2015).

[58] C. Garcia-Recio, J. Nieves, and L. L. Salcedo, SU(6) extension of the Weinberg-Tomozawa meson-baryon Lagrangian, Phys. Rev. D **74**, 034025 (2006).

[59] C. Garcia-Recio, J. Nieves, and L. L. Salcedo, Large N_c Weinberg-Tomozawa interaction and negative parity s-wave baryon resonances, Phys. Rev. D **74**, 036004 (2006).

[60] H. Toki, C. Garcia-Recio, and J. Nieves, Photon induced $\Lambda(1520)$ production and the role of the K^* exchange, Phys. Rev. D **77**, 034001 (2008).

[61] C. Garcia-Recio, L. S. Geng, J. Nieves, and L. L. Salcedo, Low-lying even parity meson resonances and spin-flavor symmetry, Phys. Rev. D **83**, 016007 (2011).

[62] D. Gamermann, C. Garcia-Recio, J. Nieves, and L. L. Salcedo, Odd parity light baryon resonances, Phys. Rev. D **84**, 056017 (2011).

[63] C. Garcia-Recio, L. S. Geng, J. Nieves, L. L. Salcedo, E. Wang, and J. J. Xie, Low-lying even parity meson resonances and spin-flavor symmetry revisited, Phys. Rev. D **87**, 096006 (2013).

[64] F. Gursey and L. A. Radicati, Spin and Unitary Spin Independence of Strong Interactions, Phys. Rev. Lett. **13**, 173 (1964).

[65] A. Pais, Implications of Spin-Unitary Spin Independence, Phys. Rev. Lett. **13**, 175 (1964).

[66] B. Sakita, Supermultiplets of elementary particles, Phys. Rev. **136**, B1756 (1964).

[67] A. J. G. Hey and R. L. Kelly, Baryon spectroscopy, Phys. Rep. **96**, 71 (1983).

[68] R. F. Dashen, E. E. Jenkins, and A. V. Manohar, The $1/\mathrm{N(c)}$ expansion for baryons, Phys. Rev. D **49**, 4713 (1994); **51**, 2489 (1995).

[69] D. G. Caldi and H. Pagels, A solution to the $\rho\pi$ puzzle: Spontaneously broken symmetries of the quark model, Phys. Rev. D **14**, 809 (1976).

[70] D. G. Caldi and H. Pagels, Spontaneous symmetry breaking and vector meson dominance, Phys. Rev. D **15**, 2668 (1977).

[71] J. Smit, Chiral symmetry breaking in QCD: Mesons as spin waves, Nucl. Phys. **B175**, 307 (1980).

[72] S. Weinberg, Pion Scattering Lengths, Phys. Rev. Lett. **17**, 616 (1966).

[73] Y. Tomozawa, Axial vector coupling renormalization and the meson baryon scattering lengths, Nuovo Cimento A **46**, 707 (1966).

[74] C. Garcia-Recio and L. L. Salcedo, $\mathrm{SU}(6) \supset \mathrm{SU}(3) \times \mathrm{SU}(2)$ and $\mathrm{SU}(8) \supset \mathrm{SU}(4) \times \mathrm{SU}(2)$ Clebsch-Gordan coefficients, J. Math. Phys. (N.Y.) **52**, 043503 (2011).

[75] J. Nieves and E. Ruiz Arriola, The $S_{11} - N(1535)$ and $N(1650)$ resonances in meson baryon unitarized coupled channel chiral perturbation theory, Phys. Rev. D **64**, 116008 (2001).

[76] L. Roca, S. Sarkar, V. K. Magas, and E. Oset, Unitary coupled channel analysis of the $\Lambda(1520)$ resonance, Phys. Rev. C **73**, 045208 (2006).

[77] D. Gamermann and E. Oset, Axial resonances in the open and hidden charm sectors, Eur. Phys. J. A **33**, 119 (2007).

[78] C. Garcia-Recio, M. F. M. Lutz, and J. Nieves, Quark mass dependence of s wave baryon resonances, Phys. Lett. B **582**, 49 (2004).

[79] T. Hyodo, D. Jido, and A. Hosaka, Origin of the resonances in the chiral unitary approach, Phys. Rev. C **78**, 025203 (2008).

[80] K. A. Olive *et al.* (Particle Data Group Collaboration), Review of particle physics, Chin. Phys. C **38**, 090001 (2014).

[81] D. Jido, J. A. Oller, E. Oset, A. Ramos, and U. G. Meissner, Chiral dynamics of the two $\Lambda(1405)$ states, Nucl. Phys. **A725**, 181 (2003).

[82] C. Garcia-Recio, J. Nieves, E. Ruiz Arriola, and M. J. Vicente Vacas, $S = -1$ meson baryon unitarized coupled channel chiral perturbation theory and the S_{01} $\Lambda(1405)$ and $\Lambda(1670)$ resonances, Phys. Rev. D **67**, 076009 (2003).

[83] J. M. M. Hall, W. Kamleh, D. B. Leinweber, B. J. Menadue, B. J. Owen, A. W. Thomas, and R. D. Young, Lattice QCD Evidence that the $\Lambda(1405)$ Resonance is an Anti-kaon-Nucleon Molecule, Phys. Rev. Lett. **114**, 132002 (2015).

[84] T. Hyodo, Structure and compositeness of hadron resonances, Int. J. Mod. Phys. A **28**, 1330045 (2013).

[85] F. Mandl and G. Shaw, *Quantum Field Theory* (Wiley, New York, 2010), p. 478.

[86] M. E. Peskin and D. V. Schroeder, *An Introduction to Quantum Field Theory* (Addison-Wesley, Reading, MA, 1995), p. 842.